Stable geometries and magnetic properties of single-walled carbon nanotubes doped with 3*d* transition metals: A first-principles study

Yosuke Yagi,[1] Tina M. Briere,[1] Marcel H. F. Sluiter,[1] Vijay Kumar,[1,2] Amir A. Farajian,[1] and Yoshiyuki Kawazoe[1]
[1]*Institute for Materials Research, Tohoku University, Aoba-ku, Sendai 980-8577, Japan*
[2]*Dr. Vijay Kumar Foundation, 45 Bazaar Street, K. K. Nagar (West), Chennai 600 078, India*
(Received 7 September 2003; revised manuscript received 11 November 2003; published 26 February 2004)

The interaction of 3*d* transition metal atoms and dimers with a single-walled armchair carbon nanotube has been investigated by first-principles density functional calculations. For Fe-, Co-, and Ni-doped (4,4) nanotubes, outside adsorption sites are the most favorable. The interactions are largely ferromagnetic for Fe and Co, with the local magnetic moments of the dimers being similar to the free dimers. However, for Ni most structures are nonmagnetic. We have also examined the effects of curvature with calculations for graphene and the (8,8) nanotube. For the (8,8) nanotube, the interaction of Co becomes more favorable inside the nanotube. Doping of a single Co atom transforms the (4,4) and (8,8) nanotubes into half-metals. These results are useful for spintronics applications and could help in the development of magnetic nanostructures and metallic nanotube coatings.

DOI: 10.1103/PhysRevB.69.075414 PACS number(s): 73.22.−f, 75.75.+a, 72.80.Rj, 73.61.Wp

I. INTRODUCTION

Single-walled carbon nanotubes (SWNTs) were first discovered in arc discharge from a carbon rod containing transition metal (TM) catalysts.[1,2] Thereafter, substantial progress has been made to synthesize SWNTs using other methods such as laser-ablation[3] or chemical vapor deposition.[4] A common feature among these methods is the requirement of a metal or a metal compound catalyst. In particular, 3*d*-TMs (Fe, Co, and Ni) are frequently used, and can mix with the nanotubes to affect their electronic and magnetic properties. This has been demonstrated by Grigorian *et al.*,[5] who observed an anomalous temperature dependence of thermopower and resistivity that varies with the metal catalyst.

Study of the interaction of metal atoms with nanotubes is important to understand their potential applications, including nanowires, high strength composites, metal coated structures, and nanoelectronic devices.[6] The interaction of magnetic atoms with nanotubes could lead to half-metallic systems that are of interest for spintronics devices[7,8] as well as nanomagnets. Such studies also provide the opportunity to investigate the magnetism of low dimensional systems. Since carbon nanotubes are ballistic conductors,[9–11] the spin polarization of the electrons induced from a magnetic electrode (such as Fe, Co, or Ni) can be preserved as the electrons propagate through the nanotube. For this aim it is necessary to know which elements can best be bonded with nanotubes and how the magnetic properties are affected. Knowledge of the bonding of metal atoms with nanotubes is also important to develop low contact resistance materials.[12]

The interactions of TM atoms with graphite or a graphene sheet have been studied both experimentally[13–17] and theoretically.[18–21] These works show that carbon p_z orbitals (π bonded states) hybridize strongly with the *d* orbitals of the TM atoms. The nanotube, however, has significant curvature, and hence its bonding picture is different from that of graphite or a graphene sheet because of σ-π hybridization.[22,23] Curvature may also lead to a coordination of TM atoms both inside and outside of the nanotube that is different from the flat graphene sheet. It is interesting to examine these effects for different dopants. Fagan *et al.*[24] studied the interaction of an Fe atom on an (8,0) semiconducting zigzag nanotube. The most stable configuration was found to be a hole site outside of the nanotube (Fig. 1) somewhat similar to an Fe atom on graphite, with magnetic moments higher for the outside configuration than the inside. In another recent study[25] adsorption of several metal atoms was considered for (8,0) zigzag and (6,6) armchair nanotubes in order to understand the variations in binding energies as well as the magnetic properties.

In the present study, we have performed first-principles calculations to clarify the interaction of 3*d*-TM atoms (Fe, Co, and Ni) on SWNTs and a graphene sheet. We have concentrated our efforts on armchair nanotubes due to their im-

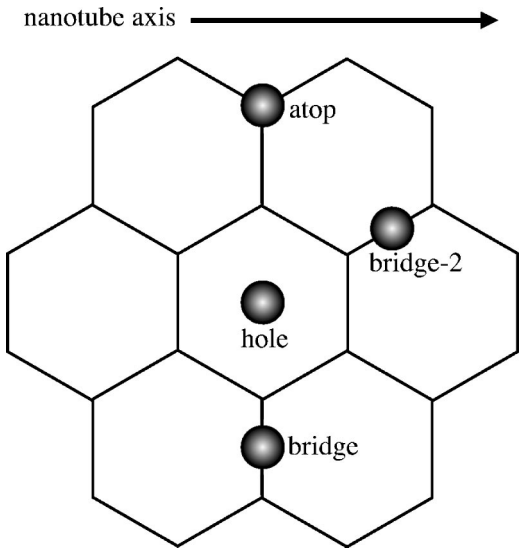

FIG. 1. Considered adsorption sites for a single atom on the graphene sheet (bridge=bridge-2) and SWNT.

portance to electron transport. In order to emphasize the effects of curvature, we have investigated the (4,4) armchair SWNT, which has a diameter of about 5.5 Å, and compared the results with those of the graphene sheet and the larger diameter (8,8) SWNT. The effects of TM atoms on the properties of SWNTs and graphene sheets and the curvature dependence of those effects have been analyzed. Finally, we briefly discuss results for the (4,4) SWNT and graphene doped with TM dimers.

II. METHOD

All calculations were performed with a spin-polarized first-principles pseudopotential plane-wave approach based on the density functional method and ultrasoft pseudopotentials.[26–28] We took the cutoff energy of the plane waves to be 287 eV for all calculations. The $3d4s$ and $2s2p$ orbitals were treated as valence states for the TMs and carbon, respectively. For the exchange-correlation energy we used the generalized gradient approximation designed by Perdew and Wang.[29]

Calculations were performed for the graphene sheet and the (4,4) and (8,8) SWNTs. All were considered as isolated and infinite in extent or length. For this purpose, we used periodic boundary conditions on supercell geometries with sufficient lateral separations among neighboring layers (10 Å) or tubes (7 Å). In order to reduce the interaction of transition metal atoms or dimers in neighboring nanotube cells, we used supercells two [4.92 Å for the (8,8) SWNT] or four [9.85 Å for the (4,4) SWNT] times larger than the unit cell in the axial direction. For the same reason, we employed a graphene supercell containing 32 carbon atoms.

Structural optimizations were performed using the conjugate gradient method. The Brillouin zone was sampled with $1\times1\times21$, $1\times1\times41$, and $9\times9\times1$ **k** points for the (4,4), (8,8), and graphene sheet calculations, respectively. The z direction was taken either along the nanotube axis or perpendicular to the graphene sheet. To improve the energy convergence we introduced partial occupancies using Gaussian broadening with a width of $\sigma=0.01$ eV. In some cases, when the calculated system was known to be metallic, we used the Methfessel-Paxton method[30] instead of the Gaussian smearing method. Structural optimizations were deemed sufficiently converged when the forces were less than 5 meV/Å.

.

III. RESULTS AND DISCUSSION

Three distinct sites were considered for a single atom on a graphene sheet, and one additional site was considered for the SWNTs. These consist of an atom (i) directly above a C atom (atop site), (ii) above the center of hexagon (hole site), (iii) over a C-C bond (bridge site), and finally (iv) an inequivalent bridge site (bridge-2 site) for the nanotubes. These sites are shown in Fig. 1. A summary of results for the stable configurations is given in Table I.

TABLE I. Summary of results for transition metal atoms on the graphene sheet and nanotubes. The binding energy (BE) per TM atom is defined by $E_{\text{pure}}+E_{\text{TM}}-E_{\text{doped}}$. The values of the magnetic moment μ are for the local magnetic moments of the transition metal atoms, i.e. the magnetic moments determined by integrating the spin over the Voronoi cells. The number of nearest carbon neighbors with the same TM-C bond length is indicated in parentheses.

	Site	BE (eV/TM)	μ_{TM} (μ_B)	TM-C dist. (Å)
graphene	Fe hole	0.99	2.1	2.12 (6), (height=1.51)
	Co hole	1.58	1.0	2.10 (6), (height=1.49)
	bridge	1.44	1.0	1.96 (2), (height=1.86)
	Ni hole	1.53	0.0	2.12 (6), (height=1.52)
	bridge	1.22	0.0	1.95 (2), (height=1.88)
(4,4) SWNT	Fe outside hole	1.33	3.1	2.14 (4), 2.41 (2)
	outside bridge-2	1.18	4.0	2.12 (2)
	outside bridge	1.15	3.9	2.08, 2.11
	inside hole	1.13	2.3	2.01 (2), 2.21 (4)
	Co outside atop	1.90	1.3	1.90, 2.08 (2), 2.30, 2.36
	outside hole	1.86	1.3	2.07 (2), 2.10 (2)
	outside bridge	1.64	1.3	1.93 (2)
	inside hole	1.61	1.0	1.95 (2), 2.16 (4)
	Ni outside atop	2.00	0.0	1.87, 2.06, 2.07
	outside hole	1.76	0.0	2.08 (2), 2.09 (2), 2.31, 2.34
	outside bridge	1.69	0.0	1.91 (2)
	inside hole	1.31	0.0	2.00 (2), 2.24 (4)
(8,8) SWNT	Co inside hole	1.65	1.1	2.02 (2), 2.12 (4)
	outside hole	1.63	1.2	2.09 (4), 2.21 (2)
	outside bridge	1.30	1.3	1.98 (2)

A. Interaction of a single atom with graphene

For graphene, we found the hole site to be the most stable for each element after optimization, while the atop site is unstable. The bridge site is also unstable for Fe. As seen in Table I, for the stable sites the TM-C distances are quite similar for all atoms. The bond lengths for the more highly coordinated hole site are longer than for the bridge site. The magnetic moments of the TM atoms on graphene are reduced by up to $2\mu_B$ relative to the free atom. The reason for this reduction, as well as others to follow, will be discussed in Sec. III D in terms of the promotion of $4s$ electrons to $3d$ states.

Two theoretical studies concerning interactions between TM atoms and graphene have been published previously.[20,21] Duffy *et al.*[20] used a linear combination of atomic orbitals molecular-orbital approach within the density functional method, where the exchange-correlation effects were included within the local spin density approximation (LSDA). Their results for the most stable sites, magnetic moments, and TM heights agree closely with our results. The binding energies of the TM atoms from our calculations are, however, smaller than theirs. This may be due to the use of the LSDA in their calculations. Aside from the subtle case of graphite,[31] local density methods tend to overestimate binding more significantly than those that incorporate gradient corrections,[32,33] and this overestimation has been seen to occur in transition metal systems.[34–36] Considering the use of pseudopotentials, the calculations of Duffy *et al.* include the $3s$ and $3p$ electrons of the TM atoms in the valence, and the good agreement with our results suggests that our approximation, including only the $3d$ and $4s$ electrons in the valence, is reasonable for this type of calculation.

On the other hand, Menon *et al.*[21] studied Ni on graphene, and found that the Ni atom exhibits a magnetic moment of $0.2\mu_B$ compared to zero found by us and Duffy *et al.* Menon *et al.* employed the tight-binding molecular dynamics method, which uses parameters fitted to experimental and *ab initio* results. Their tight-binding method requires not only parameters for the transfer integral matrix and overlap integral matrix elements, but also parameters for the interaction between the TM atoms and the graphene sheet. These parameters were obtained from density functional calculations for Ni_mC_n, $n+m \leqslant 4$ clusters. The authors obtained an energy difference of 15.4 eV for Ni at the atop and hole sites. This large difference suggests their parametrization was inadequate for the study of TM atoms on graphene.

B. Interaction of a single atom with the (4,4) SWNT

As shown in Fig. 1, four sites were considered for a single atom bound to the SWNT wall. Since the nanotube has both inside and outside surfaces, a total of 8 sites were considered.

Looking first at Fe, we see from Table I that, for inside the tube, only the hole site is stable, as the Fe atom initially placed at all other sites moves to the hole site after geometry optimization. In the case of the outside of the tube, three sites, the hole, bridge, and bridge-2, are stable upon relaxation. An Fe atom initially placed at the atop site migrates to the bridge-2 site. The hole site is the most favored. These results show some interesting differences with recent calculations on an (8,0) zigzag SWNT by Fagan *et al.*,[24] where the authors found the hole site outside of the nanotube to be the most stable (1.40 eV, with a magnetic moment of $3.9\mu_B$), followed by the atop and bridge sites. Durgun *et al.*[25] considered only the outside configurations of the (8,0) nanotube and obtained a 0.8-eV binding energy and a $2.3\mu_B$ magnetic moment for the hole site. The disparity between our results and those for the (8,0) nanotube most likely occur due to the differences in curvature for the two types of nanotubes. As seen in Table I, the magnetic moment of the Fe atom at the outside hole site is larger than the atom either the inside hole site or on the graphene sheet. From the table we can also see that the two bridge sites, which have the lowest coordination, have the highest magnetic moments. For these two sites, differences in the occupation between the majority and minority d levels are similar to the isolated atom, but for the other sites, the minority d occupation is higher, resulting in a net reduction of the magnetic moment. The band structures of the undoped and most stable inside and outside configurations of the (4,4) nanotube are shown in Fig. 2, and all are metallic. For the inside hole configuration the majority bands in the vicinity of the Fermi level are only slightly perturbed, as the TM atom derived states lie below the Fermi level. However, the minority bands show significant hybridization of the TM and nanotube states. There is an opening of a small gap just above the Fermi energy, making it close to a half-metal. For the outside hole configuration both the majority and minority bands of the nanotube have significant hybridization with the d states of the TM atom.

As with Fe doping, only the hole site is stable when a Co atom is located inside the nanotube. For the outside, three sites, the atop, hole, and bridge, are stable on relaxation. A Co atom initially placed at the bridge-2 site moves to the atop site. The magnetic moment is about $1\mu_B$ for each site, which is also the case for graphene. The atop site, which is unstable for graphene, is the most stable site; however, the energy difference between the atop and hole sites is small (0.04 eV). Therefore, it may be possible for a Co atom at the atop site to migrate to the hole site at room temperature. The binding energy of Co is significantly higher (1.90 eV) than Fe (1.33 eV). Similar behavior was obtained[25] for Co on an (8,0) nanotube, but in this case the hole site was of lowest energy. The atomic structure of the outside atop site for the (4,4) SWNT doped with a Co atom is shown in Fig. 3. One can see that Co and its neighboring carbon atoms form an sp^3-like configuration. This site also has special significance for the armchair nanotubes. The existence of the TM atom breaks the mirror symmetry of the (4,4) SWNT and lifts the degeneracy of the π and π^*bands.[37] Consequently, a small gap is generated near the Fermi level (Fig. 4). This small gap will contribute to the increasing resistivity of SWNTs at low temperature. Finally, it is very interesting that the (4,4) SWNT doped with a Co atom at the inside hole site can also be half-metallic (Fig. 2), i.e., the majority spin state is metallic, and the minority spin state is semiconducting. Half-metallic materials are important because of their unique magneto-transport properties[38] and application to spintronics devices.[39]

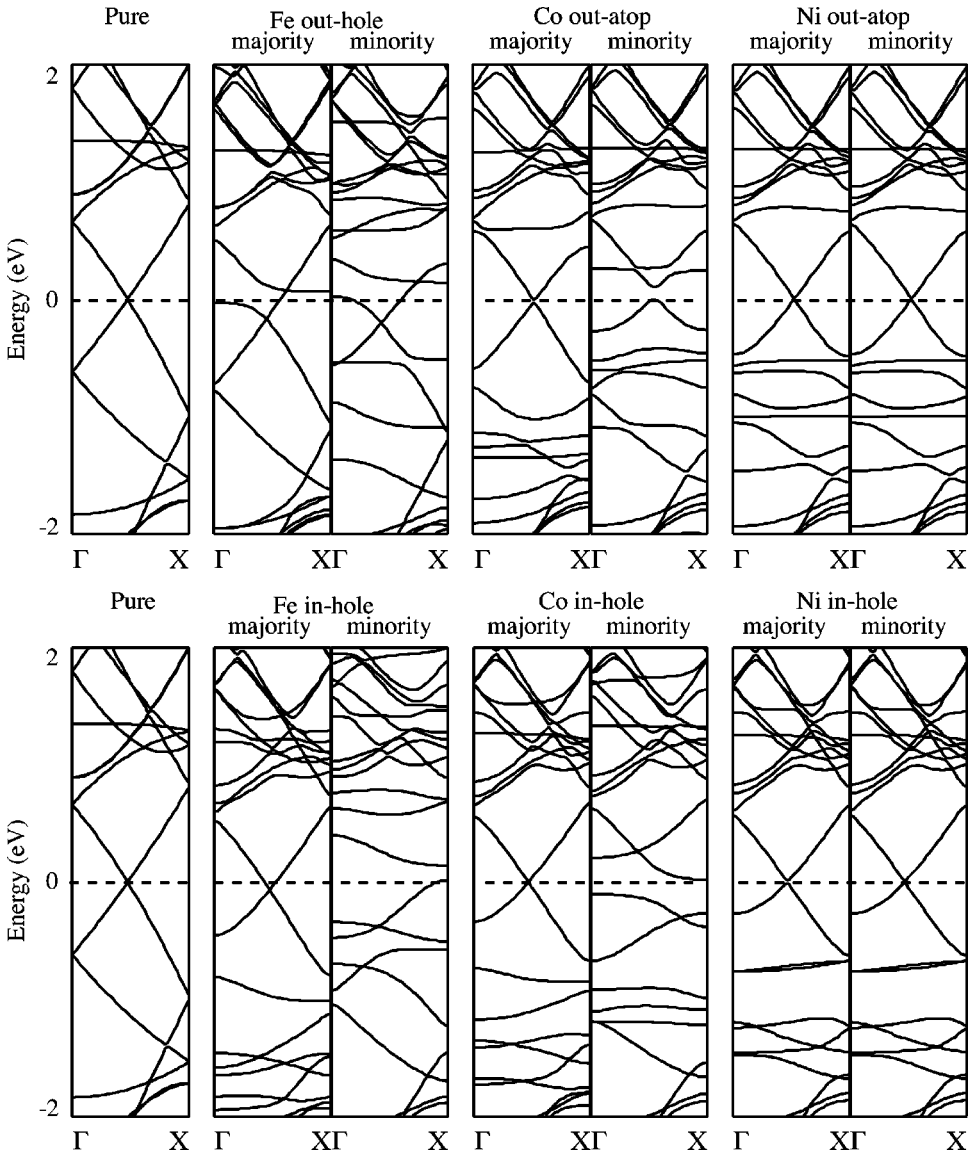

FIG. 2. Band structures for the (4,4) SWNT doped with transition metal atoms. The Fermi level ($E_F=0$) is indicated by the dashed line.

The stable sites for Ni are the same as for Co. The binding energy of Ni is similar to that of Co. Similar behavior has been obtained for Ni on an (8,0) nanotube[25] where the magnetic moment of Ni is almost fully quenched, though again the adsorption site differs. Ni at the outside atop site, which is the most stable, causes a small gap at the Fermi level (Fig. 4), as also happens with Co. Owing to the additional *d* electron contributed by the Ni atom, the identical majority and minority spin bands are more similar to the Co majority spin bands than the minority spin. These results show the interesting possibility of tailoring the properties of nanotubes by TM doping.

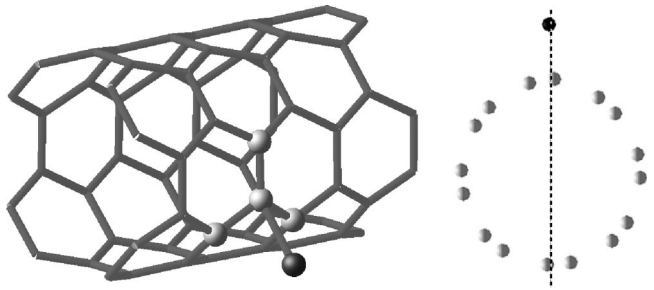

FIG. 3. Geometric structure of the outside atop site for the (4,4) SWNT doped with a Co atom; overview (right) and cross section perpendicular to the tube axis (left).

C. Interaction of Co with the (8,8) SWNT

To investigate curvature effects upon TM atom doping, we studied the (8,8) SWNT, which has a diameter twice as large as the (4,4) nanotube. Co doping is the most representative, because the Co-doped SWNTs have net magnetic moments and the adsorption sites are mostly the same as for Ni doping. Therefore, we calculated the (8,8) SWNT doped only with Co.

As mentioned earlier, we employed a supercell two times longer than the unit cell [half as long as for the (4,4) nanotube] to minimize computational time. However, the shorter interval between the TM atoms could allow for greater inter-

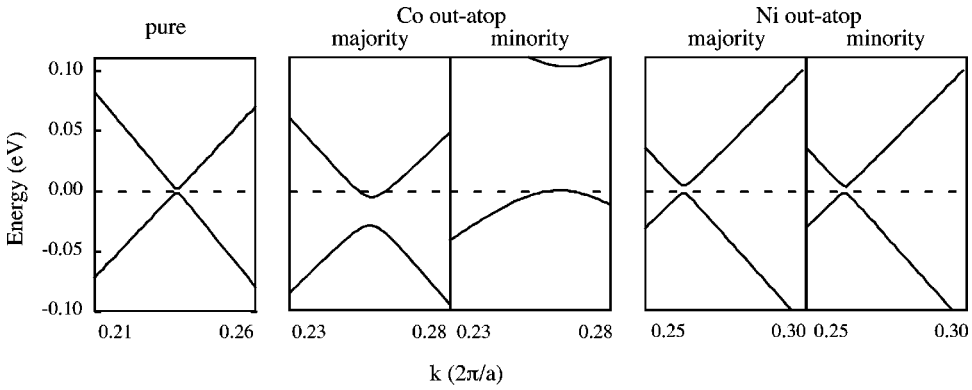

FIG. 4. Band structure near the Fermi level of the pure (4,4) SWNT, and the SWNT doped with Co and Ni at the outside atop sites. The Fermi level ($E_F=0$) is indicated by the dashed line.

actions between TM atoms in neighboring supercells. To estimate this effect, we calculated the (4,4) SWNT doped with Co using the smaller supercell (two units) and compared the results with those using the larger supercell (four units). The differences between two units and four units are shown in Table II. The TM geometries and magnetic moments are not changed significantly with the supercell length. On the other hand, the binding energy and energy gap at the Fermi level do have some differences. The difference in the binding energy (ΔBE) for the inside hole site is 0.12 eV. Also, the shorter interval between the TM atoms increases the gap and makes the (4,4) SWNT doped on the outside hole site a half-metal. Therefore, calculations for the (8,8) nanotube using two units may also be similarly affected.

As in the case with doping of the (4,4) SWNT, four inside sites and four outside sites were considered for the (8,8) SWNT. For the inside of the nanotube, only the hole site is stable, as the Co atom initially placed at all other sites moves to the hole site after geometry optimization. Outside the tube, two sites, the hole and bridge sites, are stable on relaxation. The outside atop site, which is the most stable site for the (4,4) SWNT, is unstable here. A Co atom initially placed at the atop or bridge-2 site migrates to the hole site.

The energy difference between the inside hole and outside hole sites is only 0.02 eV, with the inside site being more favorable. In contrast, for the (4,4) SWNT the difference between the two sites is 0.24 eV and the outside site is more favorable. This demonstrates one aspect of curvature. Since the (8,8) SWNT has a diameter of about 11 Å its curvature is relatively small. Therefore, the π character inside the nanotube does not significantly differ from the outside. Co doping at the inside hole and outside hole sites makes the (8,8) half-metallic with gaps of about 0.25 and 0.20 eV, respectively, in the minority spin component, similar to the (4,4) SWNT.

D. Curvature effects

The curvature dependence of the binding energy at the hole site is shown in Fig. 5. As discussed earlier, the outside of the (4,4) SWNT is the most stable for all elements, while for the inside, the relative energy varies with the type of TM atom. The preference for a TM atom to bond with a nanotube over graphene is consistent with results from x-ray diffraction experiments.[40] Fe and Co atoms favor a positive rather than zero curvature (on graphene); however, the energy of the Ni atom changes linearly with curvature. The C-C π bonds that participate in bonding with the TM atom change monotonically with the curvature (Fig. 5). Therefore, we might expect as a first approximation that the TM atom binding energy will also vary monotonically. However, the coordination number is different for the same site inside and outside of the nanotube. For instance, the inside hole site has two nearest neighbor C atoms and the outside hole site has four (Fig. 5). Therefore, the energy does not depend only on the curvature but on a more subtle interplay of curvature, preferred coordination, and magnetization energy.

Only for the Fe atom does the magnetic moment change significantly with curvature. The magnetic moments for the outside of the (4,4) SWNT are larger than those for either graphene or the inside of the nanotube. All the magnetic moments of the TM atoms except for Fe on the outside of the tube are about $2\mu_B$ lower than those of the free atoms. Duffy *et al.* examined the molecular orbitals of Fe at the hole site on graphene, and found the reduction of the magnetic moment to be caused by the promotion of the $4s$ electrons into $3d$ orbitals.[20] In a simple atomic picture, this is equivalent to the conversion of a $3d^6 4s^2$ state with a magnetic moment of $4\mu_B$ to a $3d^8$ state with a moment of $2\mu_B$. Looking at the local density of states for Fe at the inside hole and outside

TABLE II. Differences in (4,4) SWNT results obtained by using the supercells two times larger than the unit cell (two units) and four times larger than the unit cell (four units). The majority and minority band gaps (BG) are calculated separately. The difference in values is obtained from (four units)$-2\times$(two units).

	ΔBE_{4-2} (eV)	$\Delta\mu$ (μ_B)	BG, two units (eV) majority spin	BG, two units (eV) minority spin	BG, four units (eV) majority spin	BG, four units (eV) minority spin
outside atop	−0.01	0.03	~0.1	~0.1	~0.1	~0.1
outside hole	0.00	0.14	0.0	~0.2	0.0	0.0
outside bridge	−0.03	−0.05	0.0	0.0	0.0	0.0
inside hole	−0.12	0.03	0.0	~0.4	0.0	~0.1

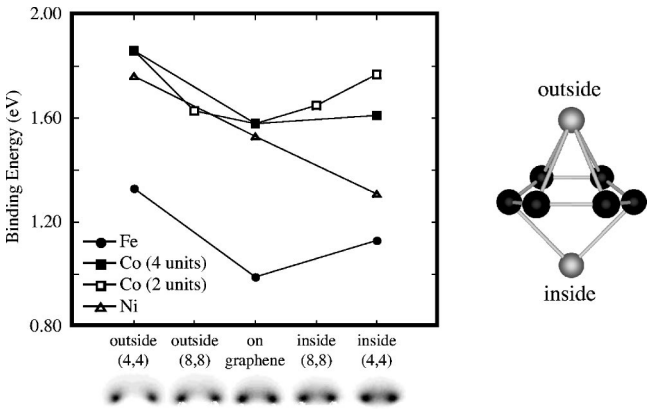

FIG. 5. Curvature dependence of the binding energy at the hole site. Figures under the horizontal axis show the charge density of the π orbital bonding with the transition metal atom. The atomic structure illustrates the difference in coordination between the inside and outside nanotube sites. Note that the hole site is not the most stable for all the systems studied here.

hole sites (Fig. 6), we can see that the states with *s* character for the inside hole site lie predominantly above the Fermi level and are thus unoccupied. The minority spin *s* character levels for the outside hole site are also unoccupied, while the corresponding majority spin levels straddle the Fermi level and are partially occupied. Thus, for the inside hole site we observe greater promotion of the $4s$ electrons into the $3d$ orbitals, resulting in a lower local moment for the inside site compared to the outside site. Similar behavior was seen by Fagan *et al.*[24] for Fe on an (8,0) nanotube.

From the above discussion we can say that a TM atom on graphene or a nanotube will generally be in a *d*-rich (*s*-poor) state. In addition to the reduction in the local magnetic moment, this also explains the smaller binding energy of Fe compared to the other TM atoms studied here. The $4s$-$3d$ interconfigurational energies for $3d$ TMs have been investigated by many researchers, both experimentally[41] and theoretically.[42,43] According to these works, the $4s$-$3d$ interconfigurational energy for Fe is larger than for Co or Ni, i.e., a *d*-rich state is unfavorable for isolated Fe. The most stable state for the TM atom bonding to graphene or a nanotube will be determined by the reduction in energy caused by bond formation and the increase in energy resulting from changes in the magnetic state. Therefore, because simply changing the magnetic state of Fe is relatively costly, the magnetic state of Fe will most easily be changed with the environment, i.e., curvature. Further, because the increasing energies resulting from the changing magnetic state for Co and Ni are small, the magnetic states can always be *d* rich, and the magnetic moments will not vary with curvature.

Finally, curvature changes the C-C bond angle of the (4,4) SWNT from 120° (as for graphene) to 119.2° and 117.8°, which is tending slightly towards the bond angles in the sp^3 configuration of diamond (109.5°). Thus, the sp^2 bonds in the (4,4) SWNT also acquire some sp^3-like character. It follows that the atop site of the (4,4) is the most stable for Co and Ni, though that of graphene or the (8,8) SWNT is unstable. In a true sp^3 configuration, the TM atom should be at the apex of the tetrahedron consisting of four C atoms. For graphene and inside the nanotube, the cost of generating this tetrahedron is large, causing the atop site to be unstable.

E. Interaction of a dimer with graphene

In order to understand the role of TM-TM interactions in TM-C bonding, we investigated dimer doping on graphene and the (4,4) SWNT. We considered three different configurations for the bonding of a TM dimer to a graphene sheet, with the TM atoms each placed at the hole, bridge, and atop sites, similar to the single atom placements. From Table III we can see that for Fe, the bridge site has the highest binding energy, while the atop site is unstable and relaxes to the bridge site. All three sites are stable for both Co and Ni. The bridge site is also most stable for Co, whereas for Ni the bridge and atop sites are nearly degenerate. These results are in good agreement with the previous local density approximation calculation,[20] except for the ordering of the Ni bridge and atop sites. All of the stable sites are favored over the isolated dimer (Table III).

The TM dimer bond lengths are elongated by 0.14–0.39 Å due to interaction with the graphene sheet. The bond lengths at the highly coordinated hole site are the longest. The shortest TM-carbon bond lengths vary between 1.99 Å (Ni atop site) and 2.25 Å (Fe hole site), with the shortest bond lengths occurring for the sites with lowest coordination. For comparison, the calculated values of the isolated dimer bond lengths are 1.97, 1.96, and 2.09 Å for Fe, Co, and Ni, respectively. Unlike single-atom adsorption, interaction of the TM dimer with the graphene sheet does not generally lead to a reduction in the dimer magnetic moments (Table III), where the free dimer moments are $3\mu_B$/atom, $2\mu_B$/atom, and $1\mu_B$/atom for Fe, Co, and Ni, respectively. This is due, in part, to the elongation of the TM dimer and

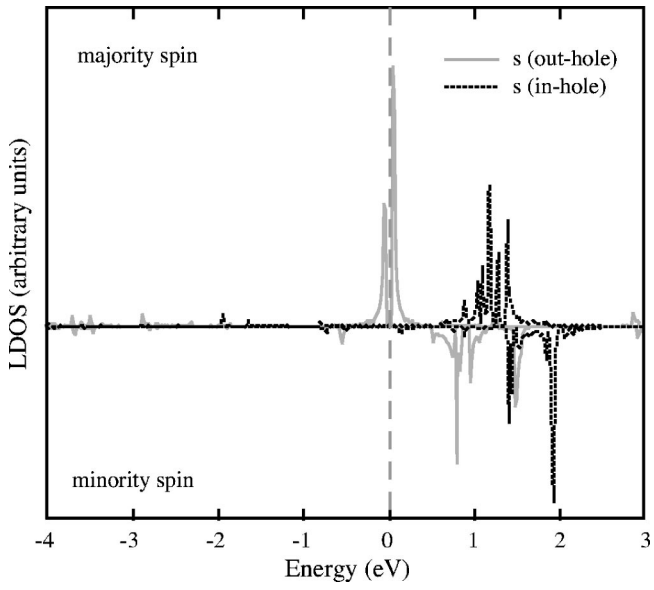

FIG. 6. Local density of states (LDOS) of Fe at the inside hole and outside hole sites of the (4,4) SWNT. The Fermi level ($E_F = 0$) is indicated by the dashed line.

TABLE III. Summary of results for transition metal dimers on a graphene sheet. The binding energy per TM atom is defined by $(E_{\text{pure}}+2E_{\text{TM}}-E_{\text{doped}})/2$. Here ΔBE is calculated with respect to the binding energies of the isolated dimers (1.56, 1.93, and 1.53 eV for Fe, Co, and Ni, respectively). The values of the magnetic moment μ are for the local magnetic moments of the transition metal atoms. The number of nearest carbon neighbors with the same TM-C bond length is indicated in parentheses. The TM-C distances are the same for both TM atoms.

Site	BE (eV/TM)	ΔBE (eV/TM)	μ_{TM} (μ_B)	TM-TM dist. (Å)	TM-C dist. (Å)
Fe bridge	1.83	0.27	3.2, 3.2	2.11	2.12, 2.17
hole	1.75	0.19	3.1, 3.5	2.22	2.25 (2), 2.31 (2)
atop	—	—	—	—	—
Co bridge	2.19	0.26	2.1, 2.1	2.08	2.09 (2)
atop	2.09	0.16	2.2, 2.2	2.08	2.05, 2.36 (2)
hole	2.04	0.11	2.1, 2.1	2.35	2.24 (2), 2.25 (2), 2.28 (2)
Ni bridge	1.85	0.32	1.0, 1.0	2.24	2.06 (2)
hole	1.84	0.31	0.0, 0.0	2.41	2.16 (2), 2.17 (2), 2.18 (2)
atop	1.78	0.25	1.0, 1.0	2.24	1.99, 2.33 (2)

TM-C bonds. The only exception occurs for the Ni hole site, where the TM-C distances are similar for both the single atom and dimer, and the magnetic moments are completely quenched.

F. Interaction of a dimer with the (4,4) SWNT

As with the single atom, the curvature of the (4,4) SWNT greatly increases the number of possible bonding sites for the TM dimer. In our calculations, we have limited the sites to four outside sites (bridge, hole, atop anti-parallel, and atop parallel) and four inside sites (straddle, atop non-aligned, hole parallel, and center). For all TM atoms, all inside sites were considered. For Ni and Co, all outside sites were also examined, while for Fe, the least likely sites from the single atom calculations were excluded. The stable optimized geometries are shown in Figs. 7–9.

For all TM atoms, the outside of the nanotube is more favorable to bonding than the inside (Table IV). The outside bridge site is most favorable for Fe. This site also has the highest binding energy for Co, while for Ni, the site with highest binding energy is the outside atop site parallel to the long axis of the nanotube. This atop site is actually a structure intermediate to a true atop or bridge site, since both TM atoms are two-fold coordinated with their carbon neighbors. The increase in binding energy compared to the single atom is due to TM-TM interactions. Relative to the free dimer and nanotube energies, all outside sites are favored (Table IV). However, for Fe, all inside sites are higher in energy, as are the Co and Ni hole parallel sites.

It is interesting that a TM atom placed inside the nanotube along its long axis (the center site) is either unstable (for Co and Ni) or has the smallest binding energy of all the sites considered (for Fe). This result suggests that formation of a one-dimensional atomic wire within the nanotube would be unlikely. However, the formation of a spiral chain (from the atop non-aligned structure) or a zigzag chain (from the straddle structure) inside the nanotube may be possible if the TM atoms could enter the nanotube. Indeed, Yang *et al.*[44] recently performed calculations for Co and Fe chains in a (9,0) zigzag SWNT and obtained large magnetic moments and high spin polarization for these structures, while Fagan *et al.*[45] studied an Fe chain on an (8,0) zigzag SWNT. Recent calculations[46] also show that Ti forms a continuous chain on a variety of SWNTs and transforms semiconducting nanotubes into metallic ones. Ti has also been found[47] to facilitate metal wire formation on nanotubes due to strong interatomic interactions.

Table IV shows that, similar to graphene, the TM dimer bond lengths for the (4,4) SWNT vary between 2.07 and 2.44 Å. Except for the center site, there is less variation in the TM-C bond lengths than for graphene. This is due to the

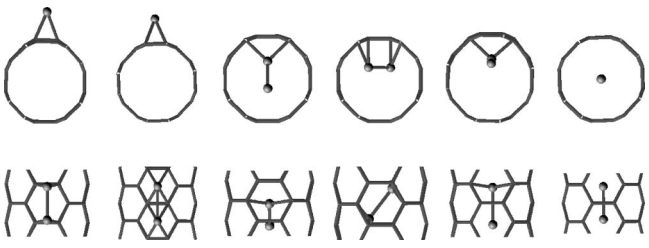

FIG. 7. Optimized configurations for the (4,4) SWNT doped with an Fe dimer. Outside: bridge and hole. Inside: straddle, atop non-aligned, hole parallel, and center.

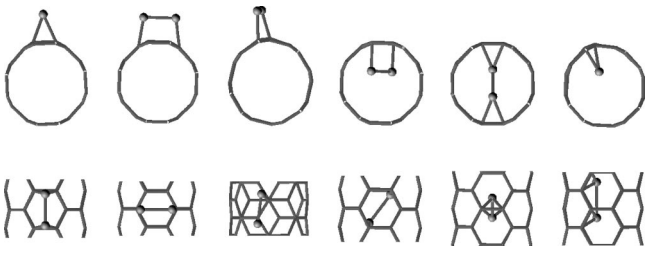

FIG. 8. Optimized configurations for the (4,4) SWNT doped with a Co dimer. Outside: bridge, atop anti-parallel, and atop parallel. Inside: atop non-aligned, straddle, and hole parallel.

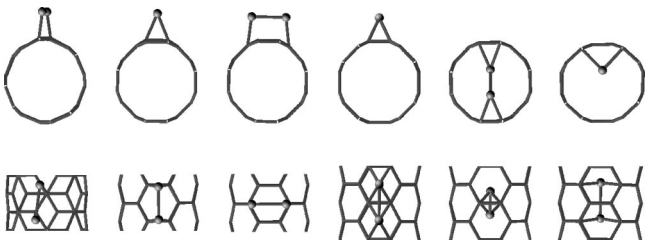

FIG. 9. Optimized configurations for the (4,4) SWNT doped with a Ni dimer. Outside: atop parallel, bridge, atop anti-parallel, and hole. Inside: straddle, and hole parallel.

curvature of the nanotube, in which there are no bonding sites with higher than four-fold coordination.

Our results show that the interactions between TM atoms are generally ferromagnetic for Fe and Co. The Ni-doped nanotubes are typically non-magnetic. The net magnetic moments ($6.2\mu_B$ and $4.0\mu_B$, respectively) of the most favored sites for the Fe and Co dimers are large and close to the free dimer values, suggesting that such TM-doped nanotubes could be useful as nanomagnets. The moments for the sites inside the nanotube are reduced or completely quenched for all TM dopants. The Fe atoms at the inside hole parallel sites have different local magnetic moments due to the asymmetry of the bonding, in which one of the Fe atoms is pulled away from the nanotube wall. Band structure calculations show that for the most favored sites the nanotubes are metallic.

The lowest energy bonding sites for the TM dimers on the nanotube are similar to those on the graphene sheet in that each dimer atom is two-fold coordinated with carbon, with similar magnetic moments for Fe and Co. The largest difference in binding energies between the most favored inside and outside nanotube sites is 0.95 eV, and for all TM atoms the binding energy varies monotonically with curvature. Unlike graphene, there is no clear trend between single atom and dimer interaction with the nanotube. For Fe, the TM-C bond lengths at the most favored dimer site are shorter than for the atom, resulting in slightly lower local moments (Table IV), while the opposite case occurs for Co. For Ni the bond lengths are nearly the same. These results illustrate the richness of the properties that can be achieved by doping with magnetic atoms.

IV. SUMMARY

In conclusion, we have studied the interaction of TM atoms on graphene and small armchair nanotubes. Our results show that curvature has a significant effect on the most favored bonding sites and magnetic moments of the TM atoms. For the single atom, the sixfold coordinated hole site on graphene is favored, but the curvature of the (4,4) SWNT leads to favored sites with lower coordination, and allows for higher magnetic moments, as in the case of Fe. Doping with

TABLE IV. Summary of results for transition metal dimers bound to the (4,4) SWNT. The binding energy per TM atom is defined by $(E_{\text{pure}}+2E_{\text{TM}}-E_{\text{doped}})/2$. Here ΔBE is calculated with respect to the binding energies of the isolated dimers (1.56, 1.93, and 1.53 eV for Fe, Co, and Ni, respectively). A negative value in ΔBE indicates the dimer-nanotube system is unbound with respect to the free dimer and isolated nanotube. The values of the magnetic moment μ are for the local magnetic moments of the transition metal atoms. The number of nearest carbon neighbors with the same TM-C distance is indicated in parentheses.

Site	BE (eV/TM)	ΔBE (eV/TM)	μ_{TM} (μ_B)	TM-TM dist. (Å)	TM1-C dist. (Å)	TM2-C dist. (Å)
Fe outside bridge	2.36	0.80	3.2, 3.2	2.15	2.06 (2)	2.06 (2)
outside hole	1.86	0.30	3.3, 3.4	2.47	2.24 (2), 2.32 (2)	2.24, 2.25, 2.29 (2)
inside straddle	1.41	−0.15	0.0, 2.9	2.20	1.97 (2),	2.17 (2) 2.05 (2), 2.26 (2)
inside atop non-aligned	1.31	−0.25	0.0,0.1	2.31	1.95 - 2.03 (4)	1.95 - 2.03 (4)
inside hole parallel	1.30	−0.26	2.3, −0.2	2.42	2.06 - 2.20 (4)	1.93 - 2.23 (6)
inside center	1.24	−0.32	3.4, 3.4	2.20	2.76	
Co outside bridge	2.69	0.76	2.1, 2.1	2.07	2.03 (2)	2.03 (2)
outside atop anti-parallel	2.64	0.71	2.0, 2.0	2.21	2.04, 2.09 (2)	2.04, 2.09 (2)
outside atop parallel	2.58	0.65	2.1, 2.1	2.11	1.99, 2.16	1.99, 2.15
inside atop non-aligned	2.03	0.10	−0.3, 0.3	2.35	1.95 - 2.05 (4)	1.95 - 2.05 (4)
inside straddle	2.02	0.09	1.1, −0.1	2.27	2.02 (2),	2.01 (2), 2.05 (2) 2.15, 2.16
inside hole parallel	1.87	−0.06	1.1, 1.1	2.40	1.98 - 2.28 (6)	1.98 - 2.31 (6)
Ni outside atop parallel	2.37	0.84	0.0, 0.0	2.37	1.90, 2.01	1.90, 2.00
outside bridge	2.29	0.76	0.1, 0.1	2.24	1.98 (2)	1.98 (2)
outside atop anti-parallel	1.75	0.22	0.4, 0.4	2.24	1.99, 2.06 (2)	1.99, 2.06 (2)
outside hole	2.02	0.49	0.0, 0.0	2.42	2.13 (3), 2.14	2.12 (2), 2.14 (2)
inside straddle	1.68	0.15	0.0, 0.0	2.34	2.07 - 2.12 (4)	2.07 - 2.12 (4)
inside hole parallel	1.44	−0.09	0.0, 0.0	2.44	2.05 - 2.17 (2)	2.06 - 2.16 (4)

TM dimers leads to lowest energy structures that have large magnetic moments for Fe and Co. Spiral and zigzag chains may form in the nanotubes if TM atoms enter the nanotube. These results may be helpful to understand further TM wire structures in nanotubes. The large moments of the Fe and Co doped structures, as well as the half-metallic behavior for certain single-atom Co doped structures, could be useful for magnetic device and spintronics applications.

ACKNOWLEDGMENTS

The authors would like to thank the staff of the Center for Computational Materials Science at the Institute for Materials Research (IMR) for computational assistance. V.K. thankfully acknowledges the kind hospitality at IMR, Tohoku University, and support from the Japan Society for the Promotion of Science (JSPS).

[1] S. Iijima and T. Ichihashi, Nature (London) **363**, 603 (1993).
[2] D.S. Bethune, C.-H. Kiang, M.S. de Vries, G. Gorman, R. Savoy, J. Vazquez, and R. Beyers, Nature (London) **363**, 605 (1993).
[3] A. Thess, R. Lee, P. Nikolaev, H.J. Dai, P. Petit, J. Robert, C.H. Xu, Y.H. Lee, S.G. Kim, A.G. Rinzler, D.T. Colbert, G.E. Scuseria, D. Tománek, J.E. Fischer, and R.E. Smalley, Science **273**, 483 (1996).
[4] J. Kong, A.M. Cassell, and H. Dai, Chem. Phys. Lett. **292**, 567 (1998).
[5] L. Grigorian, G.U. Sumanasekera, A.L. Loper, S.L. Fang, J.L. Allen, and P.C. Eklund, Phys. Rev. B **60**, R11309 (1999).
[6] A.A. Farajian, B.I. Yakobson, H. Mizuseki, and Y. Kawazoe, Phys. Rev. B **67**, 205423 (2003); K. Esfarjani, A.A. Farajian, F. Ebrahimi, and Y. Kawazoe, Eur. Phys. J. D **16**, 353 (2001); A.A. Farajian, K. Esfarjani, and Y. Kawazoe, Phys. Rev. Lett. **82**, 5084 (1999).
[7] B.W. Alphenaar, K. Tsukagoshi, and M. Wagner, J. Appl. Phys. **89**, 6863 (2001).
[8] K. Tsukagoshi, B.W. Alphenaar, and H. Ago, Nature (London) **401**, 572 (1999).
[9] L. Chico, L.X. Benedict, S.G. Louie, and M.L. Cohen, Phys. Rev. B **54**, 2600 (1996).
[10] S.J. Tans, M.H. Devoret, H. Dai, A. Thess, R.E. Smalley, L.J. Geerlings, and C. Dekker, Nature (London) **386**, 474 (1997).
[11] S. Frank, P. Poncharal, Z.L. Wang, and W.A. de Heer, Science **280**, 1744 (1998).
[12] A.N. Andriotis, M. Menon, and G.E. Froudakis, Appl. Phys. Lett. **76**, 3890 (2000).
[13] C. Binns, S.H. Baker, A.M. Keen, S.N. Mozley, C. Norris, H.S. Derbyshire, and S.C. Bayliss, Phys. Rev. B **53**, 7451 (1996).
[14] M. Bäumer, J. Libuda, and H.-J. Freund, Surf. Sci. **327**, 321 (1995).
[15] W. Branz, I.M.L. Billas, N. Malinowski, F. Tast, M. Heinebrodt, and T.P. Martin, J. Chem. Phys. **109**, 3425 (1998).
[16] A. Nakajima, S. Nagao, H. Takeda, T. Kurikawa, and K. Kaya, J. Chem. Phys. **107**, 6491 (1997).
[17] S. Nagao, T. Kurikawa, K. Miyajima, A. Nakajima, and K. Kaya, J. Phys. Chem. **102**, 4495 (1998).
[18] P. Krüger, A. Rakotomahevitra, J.C. Parlebas, and C. Demangeat, Phys. Rev. B **57**, 5276 (1998).
[19] L. Chen, R. Wu, N. Kioussis, and J.R. Blanco, J. Appl. Phys. **81**, 4161 (1997).
[20] D.M. Duffy and J.A. Blackman, Phys. Rev. B **58**, 7443 (1998).
[21] M. Menon, A.N. Andriotis, and G.E. Froudakis, Chem. Phys. Lett. **320**, 425 (2000).
[22] X. Blase, L.X. Benedict, E.L. Shirley, and S.G. Louie, Phys. Rev. Lett. **72**, 1878 (1994).
[23] O. Stéphan, P.M. Ajayan, C. Colliex, F. Cyrot-Lackmann, and É. Sandré, Phys. Rev. B **53**, 13824 (1996).
[24] S.B. Fagan, R. Mota, A.J.R. da Silva, and A. Fazzio, Phys. Rev. B **67**, 205414 (2003).
[25] E. Durgun, S. Dag, V.M.K. Bagci, O. Gülseren, T. Yildirim, and S. Ciraci, Phys. Rev. B **67**, 201401 (2003).
[26] G. Kresse and J. Hafner, Phys. Rev. B **47**, 558 (1993); **49**, 14251 (1994).
[27] G. Kresse and J. Furthmüller, Phys. Rev. B **54**, 11169 (1996).
[28] G. Kresse and J. Furthmüller, Comput. Mater. Sci. **6**, 15 (1996).
[29] J. P. Perdew, in *Electron Structure of Solids '91*, edited by P. Ziesche and H. Eshrig (Akademie Verlag, Berlin, 1991), p. 11; J.P. Perdew and Y. Wang, Phys. Rev. B **45**, 13244 (1992).
[30] M. Methfessel and A.T. Paxton, Phys. Rev. B **40**, 3616 (1989).
[31] See, for example, M.H.F. Sluiter, V. Kumar, and Y. Kawazoe, Phys. Rev. B **65**, 161402 (2002); M. Otani, S. Okada, and Z. Oshiyama, *ibid.* **68**, 125424 (2003).
[32] A.D. Corso, A. Pasquarello, A. Baldereschi, and R. Car, Phys. Rev. B **53**, 1180 (1996).
[33] D.C. Patton, D.V. Porezag, and M.R. Pederson, Phys. Rev. B **55**, 7454 (1997).
[34] T. Ziegler and J. Li, Can. J. Chem. **72**, 783 (1994).
[35] S.K. Nayak, B.K. Rao, and P. Jena, J. Phys.: Condens. Matter **10**, 10863 (1998).
[36] C.J. Barden, J.C. Rienstra-Kiracofe, and H.F. Schaefer III, J. Chem. Phys. **113**, 690 (2000).
[37] P. Delaney, H.J. Choi, J. Ihm, S.G. Louie, and M.L. Cohen, Nature (London) **391**, 466 (1998).
[38] H.Y. Hwang, S.-W. Cheong, N.P. Ong, and B. Batlogg, Phys. Rev. Lett. **77**, 2041 (1996).
[39] A.V. Khvalkovskii, A.S. Mischenko, and A.K. Zvezdin, J. Magn. Magn. Mater. **258**, 84 (2003).
[40] Z. Zhong, B. Liu, L. Sun, J. Ding, J. Lin, and K.L. Tan, Chem. Phys. Lett. **362**, 135 (2002).
[41] C. E. Moore, in *Ionization Potential and Ionization Limits from the Analysis of Optical Spectra*, *CRC Handbook of Chemistry and Physics*, edited by R.C. Weast (CRC Press, Boca Raton, FL, 1987).
[42] S. Yanagisawa, T. Tsuneda, and K. Hirao, J. Chem. Phys. **112**, 545 (2000).
[43] S. Baroni, J. Chem. Phys. **80**, 5703 (1984).
[44] C.-K. Yang, J. Zhao, and J.P. Lu, Phys. Rev. Lett. **90**, 257203 (2003).
[45] S.B. Fagan, R. Mota, A.J.R. da Silva, and A. Fazzio, Microelectron. J. **34**, 481 (2003).
[46] C.-K. Yang, J. Zhao, and J.P. Lu, Phys. Rev. B **66**, 041403 (2002).
[47] Y. Zhang and H. Dai, Appl. Phys. Lett. **77**, 3015 (2000).